

Identification of Amino Acids Controlling the Low-pH-Induced Conformational Change of Rabies Virus Glycoprotein

YVES GAUDIN,^{1*} HÉLÈNE RAUX,¹ ANNE FLAMAND,¹ AND ROB W. H. RUIGROK²

Laboratoire de Génétique des Virus, Centre National de la Recherche Scientifique, 91198 Gif sur Yvette Cedex,¹ and EMBL Grenoble Outstation, 38042 Grenoble Cedex 9,² France

Received 23 May 1996/Accepted 25 July 1996

The glycoprotein (G) of rabies virus assumes at least three different conformations: the native state detected at the viral surface above pH 7, the activated state involved in the first step of the fusion process, and the fusion-inactive conformation (I). A new category of monoclonal antibodies (MAbs) which recognized specifically the I conformation at the viral surface has recently been described. These MAbs (17A4 and 29EC2) became neutralizing when the virus was preincubated at acidic pH to induce the conformational change toward the I state of G. Mutants escaping neutralization were then selected. In this study, we have investigated the fusion and the low-pH-induced fusion inactivation properties of these mutants. All of these mutants have fusion properties similar to those of the CVS parental strain, but five mutants (E282K, M44I, M44V, V392G, and M396T) were considerably slowed in their conformational change leading to the I state. These mutants allow us to define regions that control this conformational change. These results also reinforce the idea that structural transition toward the I state is irrelevant to the fusion process. Other mutations in amino acids 10, 13, and 15 are probably located in the epitopes of selecting MAbs. Furthermore, in electron microscopy, we observed a hexagonal lattice of glycoproteins at the viral surface of mutants M44I and V392G as well as strong cooperativity in the conformational change toward the I state. This finding demonstrates the existence of lateral interactions between the spikes of a rhabdovirus.

Rabies virus is an enveloped virus which enters cells by a process of receptor-mediated endocytosis. Its negative-strand RNA genome encodes a single transmembrane glycoprotein (G) which is responsible for both virus binding to the cell surface (36) and fusion between the viral envelope and the endosomal membrane (21). G is organized in trimers (three monomers of 65 kDa each) (20, 35) and is the target of neutralizing antibodies (8).

The fusion properties of two viral strains (PV and CVS) have been investigated (19, 21). For both strains, the pH threshold for fusion is 6.3 ± 0.1 , and preincubation of the virus in the absence of a target membrane below pH 6.75 leads to inhibition of viral fusion properties. However, loss of fusion properties can be reversed by readjusting the pH to above 7. This is the main difference between rhabdoviruses (such as rabies virus) and viruses fusing at low pH from other viral families, for which low-pH-induced fusion inactivation is irreversible (18).

We have previously demonstrated that G can assume at least three different states (19, 21): the native (N) state detected at the viral surface above pH 7; the activated (A) hydrophobic state, which interacts with the target membrane as a first step of the fusion process (12); and the fusion-inactive conformation (I). There is a pH-dependent equilibrium between these states, the equilibrium being shifted toward the I state at low pH. The different conformations have been characterized by using different biochemical and biophysical techniques (19, 21). The A state is detected immediately after acidification and induces the formation of viral aggregates stabilized at low pH and low temperature. The I state is detected after prolonged incubation at low pH. In the I conformation, G is longer than

in the N conformation and also antigenically distinct and more sensitive to proteases.

The role of the I state during the viral cycle was unclear. Comparison of the kinetics of the conformational change toward the I state with those of fusion for two rabies strain (PV and CVS) has shown that although the PV strain fuses faster, inactivation and the conformational change of its glycoprotein occur more slowly than for the CVS strain. This finding suggested that the structural transition toward the I state is irrelevant to the fusion process. Results from immunofluorescence experiments with monoclonal antibodies (MAbs) directed against G suggested that G is transported through the Golgi apparatus in a non-N conformation, probably in an I state-like conformation. It then acquires its native structure near or at the cell surface. We have therefore proposed that the role of the I state is to avoid unspecific fusion during transport of G in the acidic Golgi vesicles (21).

In vesicular stomatitis virus (VSV), another rhabdovirus, the same three states (i.e., N, A, and I) have been postulated on the basis of kinetic studies (7, 27). After incubation at low pH, the quaternary structure of VSV glycoprotein is stabilized (11) and the glycoprotein appears to be more resistant to trypsin (15). A monomeric soluble form of VSV G, cleaved from virus with cathepsin D, has also been shown to acquire hydrophobic properties when incubated at low pH (9). Although it is not known whether these different conformations of the VSV glycoprotein are associated with fusion or fusion inactivation, these results suggest that rabies virus and VSV glycoproteins behave rather similarly. Finally, although the region interacting with the target membrane during the fusion process (the so-called fusion peptide) is now well delimited for both rabies virus and VSV (12, 14, 15, 24, 38), nothing is known about the region of the glycoprotein which controls its conformational change.

We have recently described two MAbs (17A4 and 29EC2) which bound native and inactive rabies virus G at the cell

* Corresponding author. Phone: 33 1 69 82 38 37. Fax: 33 1 69 82 43 08. Electronic mail address: Yves.Gaudin@cnsr-gif.fr.

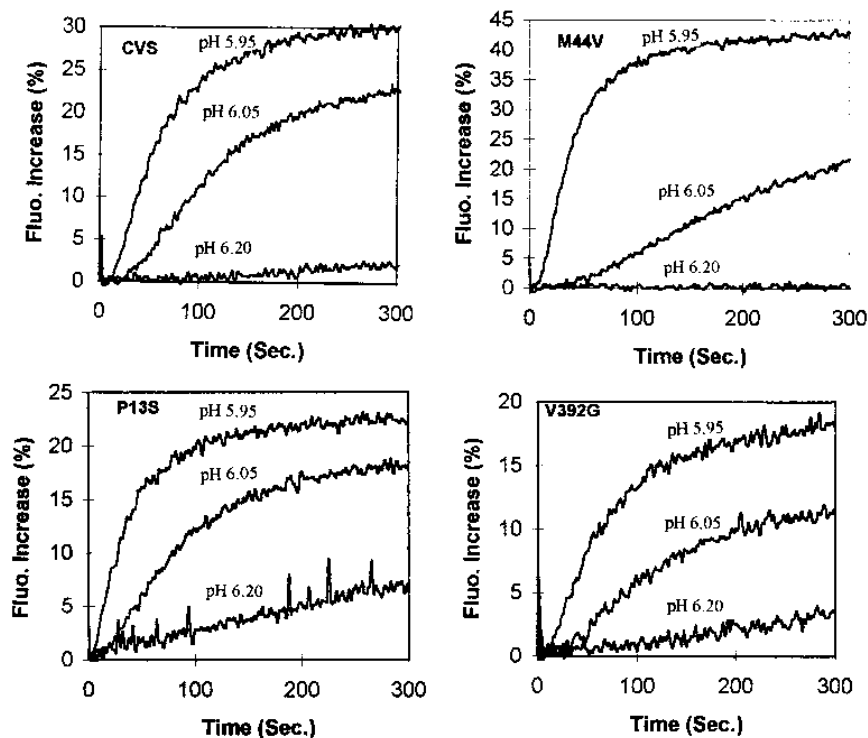


FIG. 1. Fusion characteristics of the CVS strain and RAIN mutants P13S, M44V, and V392G with liposomes. Experiments were performed at 23°C and the indicated pHs as described in Materials and Methods. Flu., fluorescence.

surface or after detergent solubilization with equal efficiency but recognized only the I conformation of G on the viral surface (21, 28). These antibodies became neutralizing when the virions were preincubated at pH 6.4 and 37°C for 2 h, after which about 90% of the spikes were in the I state (28). It was then possible to select antigenic mutants escaping neutralization. These mutants were called RAIN (resistant to acid-induced neutralization) mutants. Eleven different RAIN mutants were selected (28). The mutations were not localized in previously defined antigenic sites (1, 26, 31) and were rather dispersed along the primary sequence (mutations in amino acids [aa] 10, 13, 15, 44, 282, 392, and 396). In this study, we have investigated the fusion properties of the RAIN mutants as well as their conformational changes at low pH. We show that the epitopes for the two antibodies contain aa 10, 13, and 15 and that mutations in aa 44, 282, 392, and 396 affect the structural transition toward the I state. Furthermore, at the surface of mutants M44I and V392G, we have detected a hexagonal lattice. This latter result demonstrates for the first time the existence of lateral interactions between the spikes of a rhabdovirus.

MATERIALS AND METHODS

Chemicals. *N*-(Lissamine rhodamine B sulfonyl) (RHO)-phosphatidylethanolamine (PE) and *N*-(7-nitro-2,1,3-benzoxadiazol-4-yl) (NBD)-PE were purchased from Avanti Polar Lipids, Inc. (Birmingham, Ala.). Phosphatidylcholine, PE, gangliosides (type III from bovine brain), and cholesterol were supplied by Sigma Chemicals Co. [1 α ,2 α (n)-³H]cholesterol was obtained from Amersham.

Viruses and MAbs. The CVS strain of rabies virus and the derived RAIN mutants, K10E, K10N, P13L, P13S, S15N, S15I, S15R, M44I, M44V, E282K, V392G, and M396T (28), were cultivated on BSR cells (a clone of BHK-21 cells) and purified as previously described (20). After purification, the virus was resuspended in TD (137 mM NaCl, 5 mM KCl, 0.7 mM Na₂HPO₄, 25 mM Tris-HCl [pH 7.5]). MAbs 17A4 and 29EC2 were previously characterized (21, 28). They were used as mouse ascites preparations.

Preparation of liposomes and assays for fusion and low-pH-induced inacti-

vation. A total of 600 μ g of phosphatidylcholine, 300 μ g of PE, and 100 μ g of gangliosides dissolved in organic solvents were mixed with 10 μ g of RHO-PE and 10 μ g of NBD-PE and dried in vacuo. After addition of 1 ml of 150 mM NaCl, the mixture was sonicated for six 3-min periods in a bath sonicator. The liposome suspension was clarified at 3,500 \times g for 5 min, and the supernatant was used in the subsequent assay. Fusion was assayed as previously described (19, 21). Briefly, 10 μ g of fluorescent liposomes was mixed with about 50 μ g of virus in a buffer containing 150 mM NaCl and 5 mM Tris-HCl (pH 7.5) (final volume, 600 μ l) in the cuvette of a thermostated Perkin-Elmer LS50B spectrofluorimeter. After 5 min of incubation at 23°C, 400 μ l of phosphate-citrate buffer at the required pH (prepared from 100 mM citric acid–200 mM dibasic sodium phosphate solution) was added, and the increase of NBD fluorescence was monitored continuously. Excitation was at 455 nm (slit width, 4 nm), and emission was at 535 nm (slit width, 10 nm). The mixture was kept under continuous stirring during the experiment. For studies of the kinetics of low-pH-induced viral inactivation, the virus was preincubated at the required temperature and pH and then directly diluted in the cuvette containing the liposomes in the fusion buffer at pH 5.95. The fraction of residual activity was then determined by dividing the increase of fluorescence at the plateau by the increase of fluorescence at the plateau of the control (i.e., fusion of virus without preincubation). To obtain the time of half-inactivation at pH 6.05 and 37°C, the logarithm of the fraction of residual activity was plotted as a function of the time of preincubation at pH 6.05 and 37°C. This way of plotting gave a straight line ($r > 0.985$ for each mutant tested) and thus allowed an easy calculation of the time of half-inactivation.

Liposome binding to virus. For these experiments, liposomes were made of phosphatidylcholine, PE, and cholesterol in a 2/1/1 weight ratio. One microcurie of tritiated cholesterol was added per mg of lipid. The final lipid concentration was 1 mg/ml. For binding experiments, about 50 μ g of virus were added to 5 μ l of radioactive liposomes. The volume was completed up to 150 μ l by adding TD buffer (pH 7.5) or phosphate-citrate buffer at pH 6.4 or 6.7. The mixture was incubated for 5 min on ice, layered onto a 25% glycerol solution in TD buffer or phosphate-citrate buffer at the required pH, and then centrifuged for 50 min at 40,000 rpm in an SW55 rotor (Beckman). The fraction of liposomes associated with virus in the pellet was determined by liquid scintillation counting. In the absence of virus, less than 0.3% of the total radioactivity was found in the pellet.

RAIN mutant neutralization at pH 6.4. To assay virus neutralization at pH 6.4, the virus was first diluted in a 120 mM NaCl phosphate-citrate buffer (pH 6.4) (prepared from 10 mM citric acid–20 mM dibasic sodium phosphate solution) and incubated for 2 or 16 h at 37°C. Then 100 μ l of virus was incubated with 20 μ l of the appropriate antibody for 1 h and room temperature. The virus-antibody mixture was serially diluted in saline buffer (pH 7.4) for a plaque assay.

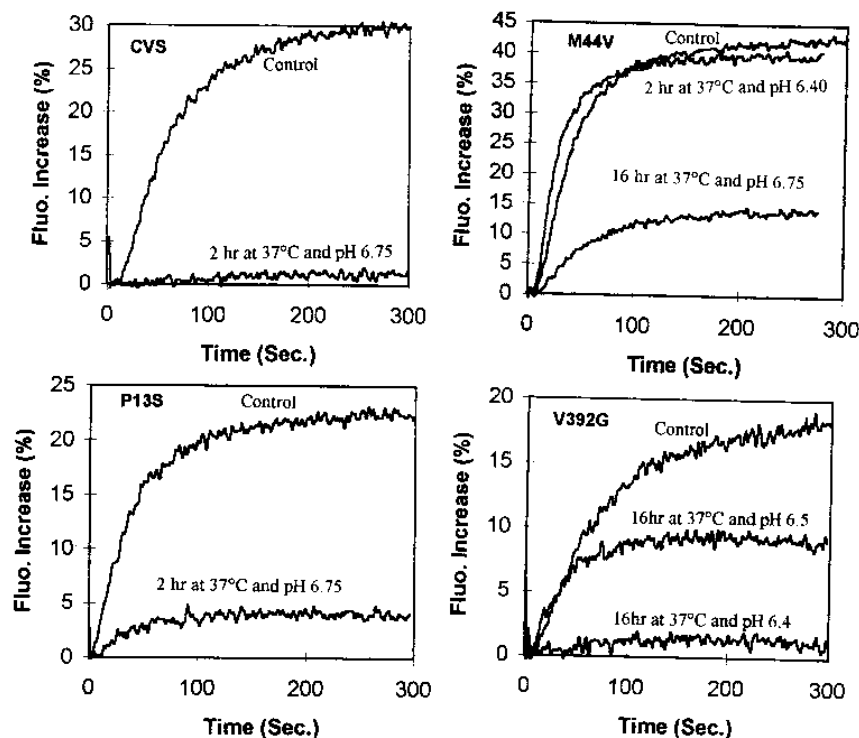


FIG. 2. Inactivation of the fusion properties of the CVS strain and RAIN mutants P13S, M44V, and V392G at acidic pHs. Virus pretreated at the indicated pHs for the indicated times was added to a cuvette containing liposomes (final pH, 5.95). Control, fusion of untreated virus with liposomes at pH 5.95; Fluo., fluorescence.

EM. Virus was observed by electron microscopy (EM) after negative staining with 1% sodium silicotungstate as described previously (20). Estimates of percentage of spikes in the I conformation were made both from direct observation of the sample in the microscope and from low-dose pictures taken randomly. The two estimates agreed within 15%.

RESULTS

Fusion characteristics of RAIN mutants. The resonance energy transfer method of Struck et al. (32) was used to assay for fusion. For the parental strain (CVS) and all of the RAIN mutants, the fusion rate and the fusion extent were maximal below pH 6. Figure 1 shows typical fusion curves for the parental strain and three RAIN mutants. All of the mutants were able to fuse with target liposomes at pH 6.05 and had a pH threshold above which no fusion was detected at pH 6.2 to 6.3. Therefore, the mutants have fusion properties similar to those of the parental strain.

The kinetics of low-pH-induced fusion inactivation of the RAIN mutants were then compared with those of the parental strain. Figure 2 shows the residual fusion activity at pH 5.95 after 2 and 16 h of preincubation at pH 6.4 or 6.75 and 37°C for the same viruses as used in the study shown in Fig. 1. The complete results are summarized in Table 1. Two categories of mutants could be distinguished. Category A contained the mutants with mutations located at positions 10, 13, and 15, which were inactivated after 2 h of preincubation at 37°C at pH 6.75 or 6.4. Some of these mutants (particularly S15R and S15I) were inactivated faster than the parental strain at pH 6.05. Category B contained the mutants with mutations located in aa 44, 282, 392, and 396, which kept their fusogenic properties almost intact after 2 h of preincubation at pH 6.75 or 6.4 and 37°C. Three of these mutants also showed a significant increase of their times of half-inactivation at pH 6.05 and 37°C. Prolonged incubations (16 h at 37°C) at pH 6.75 were necessary to

inactivate the fusion properties of M44V, M44I, and E282K, whereas lower pHs were necessary to inactivate V392G and M396T under the same conditions. Antigenic mutants selected with MAbs directed against antigenic site II or III (26, 31) (category C) were also tested in the same assay (Table 1). They show roughly the same properties as the parental CVS strain. As for the CVS strain (19, 22), for all mutants tested, fusion inactivation was reversed after reincubation of the virus above pH 7, indicating that fusion inactivation was not due to glycoprotein denaturation after prolonged incubation at low pH.

As previously observed when the CVS and PV strains were compared (21), there was no correlation between the kinetics of fusion and those of inactivation, confirming our hypothesis that the conformational change leading to inactivation is not related to the fusion process.

Finally, mutations at positions 44, 282, 392, and 396 slowed the kinetics of the conformational change toward the I state or shifted the equilibrium toward the N state at a given pH. For these mutants, not enough spikes were in the I state after 2 h at pH 6.4 to allow sufficient antibody binding to neutralize the virus (13). We can also postulate that aa 10, 13, and 15 are located in the epitopes recognized by both MAbs 29EC2 and 17A4 and that mutations in these positions allow the mutant to escape neutralization by decreasing the affinity of the MAbs for G. The following experiments were performed to confirm this hypothesis.

Neutralization of the RAIN mutants by MAbs 17A4 and 29EC2. We investigated the sensitivity of RAIN mutants to MAbs 17A4 and 29EC2 after preincubation of virus at pH 6.4 and 37°C for 2 or 16 h (Table 2). As previously observed (28), mutants with mutations located at positions 44, 392, and 396 were resistant to both MAbs after 2 h of preincubation at pH 6.4, while mutants with mutations located in aa 10, 13, and 15

TABLE 1. Kinetics of low-pH-induced fusion inactivation of various mutants of the CVS strain^a

Category	Virus	Time of half-inactivation at pH 6.05	Residual activity (%)				
			After 2 h at:		After 16 h at:		
			pH 6.75	pH 6.4	pH 6.75	pH 6.5	pH 6.4
A	CVS	4 min	<5				
	K10E	8 min	47	<5			
	K10N	2 min	<5				
	P13L	1.5 min	<5				
	P13S	3 min	20	<5			
	S15N	3.5 min	<5				
	S15I	40 s	<5				
B	M44I	35 min	>90	>90	19	<5	
	M44V	61 min	>90	>90	34	<5	
C	E282K	9 min	>90	64	<5		
	V392G	33 min	>90	>90	>90	55	<5
	M396T	8 min	>90	>90	>90	71	<5
	G34E	4 min	<5				
	I36T	4 min	<5				
C	G40E	5 min	12.5				
	S42F	7.5 min	<5				
	R184G	4.5 min	<5				
	K198E	6 min	<5				
	R333Q	4 min	ND				

^a Preincubations were performed at 37°C. Experiments and calculations of residual fusion activity and time of half-inactivation at pH 6.05 were done as described in Materials and Methods. Mutants were classified in three categories according to their origins and properties: A, RAIN mutants with kinetics of inactivation similar to (or faster than) those of the CVS strain; B, RAIN mutants with slower kinetics of inactivation; and C, antigenic mutants from sites II and III (26, 31).

were resistant only to the MAb used for their selection (except S15R and P13S, which were resistant to both). After 16 h of preincubation at pH 6.4, the pattern of sensitivity to both MAbs was the same as after 2 h of preincubation for the mutants with mutations located at positions 10, 13, and 15, whereas the mutants with mutations located in aa 44, 392, and 396 were neutralized by both MAbs.

TABLE 2. Neutralization of RAIN mutants by MAbs 17A4 and 29EC2^a

Mutant	Neutralization			
	2 h, pH 6.4, 37°C		16 h, pH 6.4, 37°C	
	17A4	29EC2	17A4	29EC2
K10E ^b	-	+	-	+
K10N ^b	-	+	-	+
P13L ^b	-	+/-	-	+/-
P13S ^c	-	-	-	-
S15I ^b	-	+/-	-	+/-
S15N ^b	-	+	-	+
S15R ^c	-	-	-	-
M44I ^c	-	-	+/-	+/-
M44V ^c	-	-	+	+
V392G ^b	-	-	+	+
M396T ^b	-	-	+	+

^a The virions were preincubated for 2 or 16 h at pH 6.4 and 37°C before addition of the MAbs. Experiments were performed as described in Materials and Methods. -, more than 60% survivors; +/-, between 10 and 60% survivors; +, less than 10% survivors.

^b Mutant selected by MAb 17A4.

^c Mutant selected by MAb 29EC2.

TABLE 3. EM observations of low-pH-incubated CVS virus and RAIN mutants^a

Virus	Duration and temp (°C) of incubation	% of spikes in the I state and aggregation state after each incubation ^b			
		pH of incubation			
		6.75	6.6	6.4	6.0
CVS	5 min, 0	N, +/-	N, +/-	N, ++	
	2 h, 37	50, -		80, -	100, +
K10E	5 min, 0	N, +/-		N, ++	
	2 h, 37	50, -		90, +/-	
P13L	5 min, 0	N, +/-		N, +	
	2 h, 37	50, -		90, -	
S15N	5 min, 0	N, +/-		N, ++	
	2 h, 37	50, -		80, -	
M44I	5 min, 0	N, -	N, +/-	N, ++	
	2 h, 37	10, -	10, -	20, -	80, -
	16 h, 37	30, -	50, -	80, -	
V392G	5 min, 0	N, -	N, +/-		
	2 h, 37	10, -	10, -	10, -	90, -
	16 h, 37	30, -	50, -	80, -	
M396T	5 min, 0	N, +/-	N, +		
	2 h, 37	N, -	N, -	N, -	100, +
	16 h, 37	10, -	30, -	80, -	

^a The various viruses were incubated at the indicated pH and temperature for the indicated times. The samples at 0°C were incubated for 5 min only since it was previously observed that aggregates process occurs very fast at this temperature (19).

^b N, all spikes were in the N conformation; -, no aggregation; +/-, beginning of aggregation; + aggregation; ++, massive aggregation.

These results are consistent with our hypothesis. They indicate that MAbs 17A4 and 29EC2 are able to neutralize mutants with mutations located at positions 44, 392, and 396 provided that they are preincubated at pH 6.4 for a long enough period of time to allow the conformational change of a sufficient number of spikes. These experiments also showed that MAbs 17A4 and 29EC2, although directed against the same region of the protein containing aa 10 to 15, did not recognize exactly the same epitope.

EM. Using negative-stain EM, we previously showed (19, 21) that incubation of different viral strains below pH 6.7 resulted in massive viral aggregation reflecting the existence of spikes in the A state (12, 19). Viral aggregates were stabilized in the cold and were not detected above pH 6.3 at 37°C. Longer incubation resulted in the appearance of long and wavy spikes which were in the I conformation. These features were also investigated for the RAIN mutants.

Observation of mutants K10E, P13L, and S15N showed that they behaved exactly like the CVS parental strain (Table 3). The virions were aggregated below pH 6.7 at 0°C. This aggregation was less extensive at higher temperatures. About 50% of the spikes were in the lengthened I state after 2 h at pH 6.7 and 37°C. This proportion reached 80 to 90% after 2 h at pH 6.4 and 37°C.

For mutants M44I, V392G, and M396T, the aggregation phenomenon was less extensive. Particularly, and differently from the CVS parental strain, at pH 6.7 and 0°C but also at pH 6.0 and 37°C, no aggregates were observed in the cases of M44I and V392G. For these three mutants, the appearance of the lengthened spikes was also considerably delayed. After 2 h at pH 6.7, 6.6, or 6.4, only few spikes had changed. Even after 16 h of incubation at pH 6.7, the extent of the conformational change was less important than that for the parental strain. This was particularly noticeable for M396T, for which only 10% of the spikes were changed. However, after 16 h of incu-

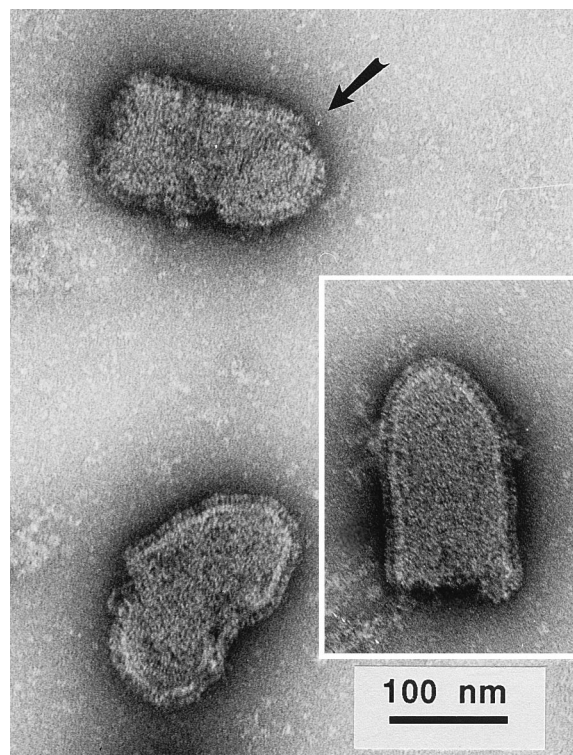


FIG. 3. Electron micrograph of negatively stained M44I RAIN mutant virus after incubation for 2 h and 37°C and pH 6.7. Note that from the three virions taken from the same EM picture, two are completely covered by native G protein 8.3 nm long (20), which is well defined and can be seen to form a dark line close to the viral membrane corresponding to the thin stalk and a whiter line more distal corresponding to the head. The third virion, indicated by an arrow, is totally covered by spikes in the I form which are less well defined, more wavy, and slightly longer (11.5 nm [19]).

bation at 37°C and pH 6.4, about 80% of the spikes were changed for the three mutants. Therefore, these EM estimates of the extent of the conformational change from N to the I conformation were in good agreement with the results obtained in fusion inactivation experiments.

Furthermore, EM observations of M44I revealed that the conformational change toward the I conformation of G was cooperative: even after only 2 h of incubation at pH 6.7 and 37°C, some virions appeared to have all of their glycoproteins in the I state, whereas most of the virions were unchanged (Fig. 3). This feature had not been detected before, although careful observations of the other RAIN mutants and of the CVS parental strain did indicate that the inactive glycoproteins were always grouped and not randomly dispersed at the viral surface. Therefore, the cooperativity of the conformational change of rabies virus glycoprotein may be a general feature and not a particularity of mutant M44I, although it is more strongly observed with this mutant.

Another unexpected result was the observation of a hexagonal lattice of glycoproteins at the surface of mutants M44I (Fig. 4) and V392G. Each angle of a hexagon is probably made up by a trimer of G (seen as three dots at the viral surface) as presented in the model in Fig. 4. The lattice was probably not very stable since it was not observed at the surface of all virions. This phenomenon was most pronounced with M44I and seemed to be strongly stabilized at slightly acidic pH (6.6) and 0°C. However, it was never observed under experimental conditions in which we detected spikes in the I confor-

mation, suggesting that the structural transition toward the I state disrupts this spike organization. Despite careful observations, we did not detect such a lattice at the surface of the other mutants or the CVS parental strain.

Virus-liposome interaction. We have previously shown that in the case of the CVS and PV strains, aggregation reflected the presence of glycoproteins in an activated hydrophobic state at the viral surface (12, 19, 21). Therefore, the lack of aggregation of mutant M44I and V392G at pH 6.7 on ice and at pH 6.0 and 37°C was intriguing. We decided to investigate directly virus-liposome interaction. The virus was incubated with liposomes containing traces of tritiated cholesterol at pH 7.4, 6.7, or 6.4 for 5 min on ice, layered on top of a 25% glycerol solution at the same pH, and centrifuged. The fraction of liposomes associated with the virions was then determined by liquid scintillation counting. Just like the parental strain, mutants M44I and V392G showed an increase in interaction with liposomes at acidic pH (Table 4). Thus, these mutants are also able to expose their hydrophobic peptides at pH 6.7, although this exposition does not lead to viral aggregation.

DISCUSSION

We have previously described a new category of anti-G MAbs which recognize specifically the I state of the glycoprotein at the viral surface (28). These MAbs were neutralizing when they were incubated for longer periods (16 h at room temperature) or at higher temperature (1 h at 37°C) with virus at pH above 7. They were also neutralizing when the virus was preincubated at pH 6.4 and 37°C for 2 h in order to induce the conformational change toward the I state of G. Therefore, we were able to select a new class of mutants (RAIN mutants) escaping neutralization by those MAbs (28). A priori, two categories of RAIN mutants might exist. The first group might be composed of mutants with a decreased affinity for the MAb; the second group might be composed of mutants with altered conformational change properties. The results presented here show that it is indeed the case.

The most simple explanation of how mutations in aa 10, 13, and 15 allow the virus to escape neutralization is that they decrease the affinity of the MAbs for the virus. Therefore, aa 10, 13, and 15 probably belong to the binding sites of MAbs 17A4 and 29EC2. The epitope recognized by these MAbs is not accessible on the native molecule on the viral surface. However, once the glycoprotein is solubilized, these MAbs bind the N state of G as well as the I state (21). This finding suggests that the region from aa 10 to 15 is located underneath the head of the glycoprotein (20) and that, because of the high concentration of G in the viral membrane, steric hindrance inhibits interaction of MAbs 17A4 and 29EC2 with native G at the viral surface. The role of this amino-terminal region is unknown. However, mutants S15I and S15R are inactivated about six times faster than the CVS strain at pH 6.05 (Table 1).

TABLE 4. Virus-liposome interactions^a

Virus	% of virion-associated liposomes in pellet after incubation at pH:		
	7.4	6.7	6.4
CVS	2.2	12.7	20.7
M44I	1.4	6.6	21.1
V392G	1.3	16.3	34.6

^a Incubations were performed on ice as described in Materials and Methods.

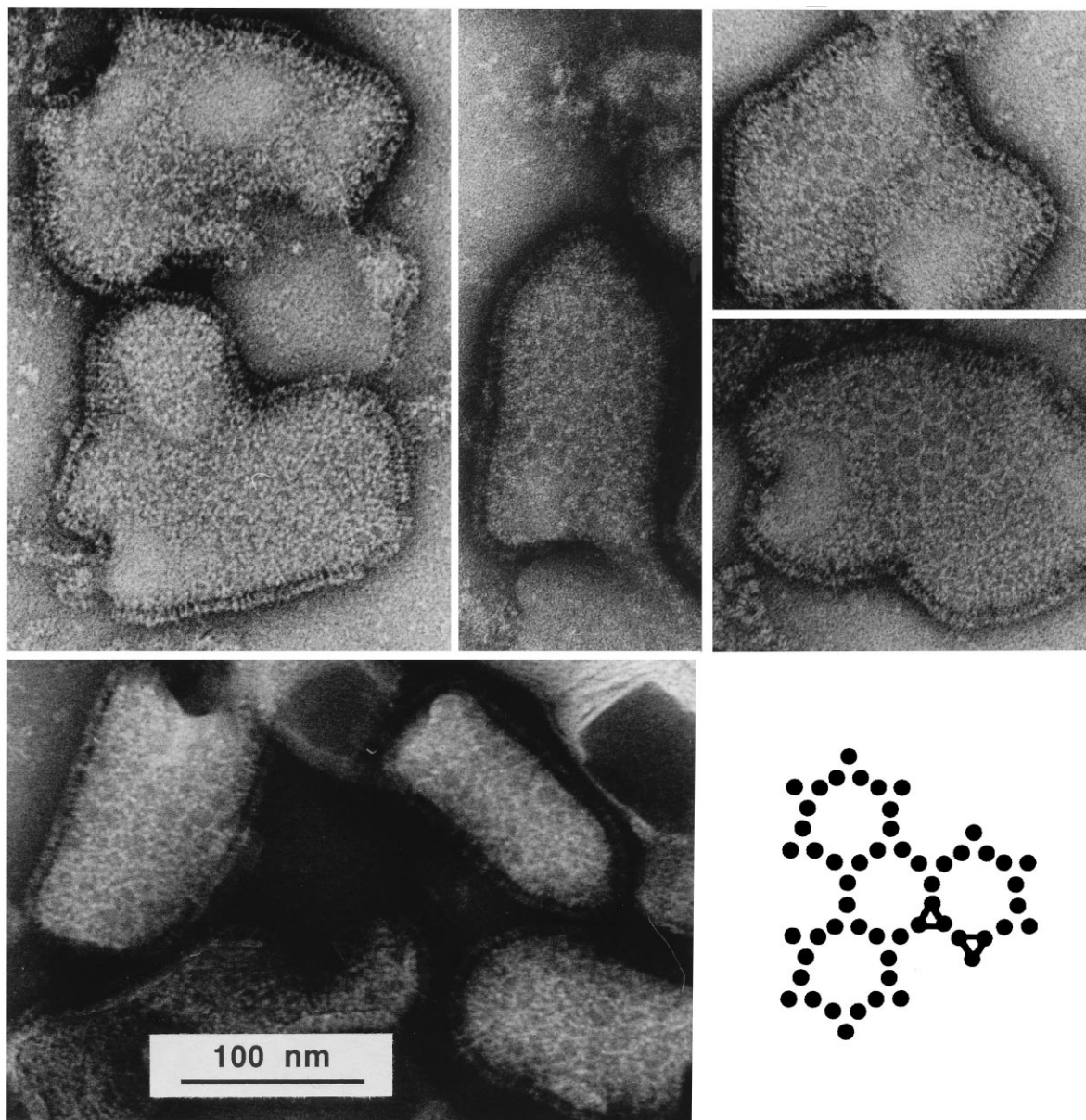


FIG. 4. Electron micrographs of selected M44I RAIN mutant virus particles negatively stained after a preincubation at pH 6.7 and 0°C. Note the hexagonal lattice on the viral surface. The two particles at the top left clearly show trimeric spikes that are beginning to self-associate in a lattice but are still largely disordered. All micrographs have the same magnification, indicated by the bar. The drawing suggests how G could associate to form these lattices; two trimers are indicated with a triangle for clarity.

Therefore, residue 15 may play a role in the overall stability of the N state of G.

The mutations in aa 44 and 282 affect the kinetics of the conformational change toward the I state, whereas mutations in aa 392 and 396 also modify the thermodynamic equilibrium between the N and I states at a given pH. Although the structural transition of these mutated glycoproteins toward the I state is affected, we have not been able to detect any significant difference in their fusion properties. Therefore, these results reinforce the idea that the transition toward the I state is irrelevant to the fusion process (12, 21), although, as mentioned previously (21), alternative explanations cannot be excluded because these results were obtained in a liposome assay lacking several elements of the normal infection route.

Amino acid 44 is located near antigenic site II, which is known to be disrupted by the structural transition toward the I state (19). However, aa 44 does not belong to this antigenic site, as mutants M44V and M44I are still neutralized by the antibodies recognizing antigenic site II (28). Reciprocally, mutations in aa 34, 36, 40, and 42, which are located in antigenic site II (26), do not affect significantly the characteristics of the structural transition toward the I state (Table 1).

Amino acids 392 and 396 are located near histidine 397 and proline 398, which are conserved among all rhabdovirus glycoproteins (Fig. 5). This region is located between two putative amphipathic alpha helices (predicted more or less strongly for all rhabdoviruses [Fig. 5]) which may partially constitute the previously described tail of G (20). Histidine 397 and proline

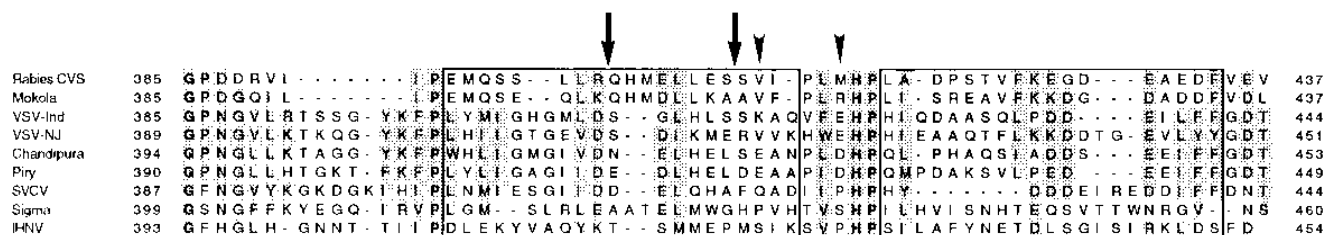


FIG. 5. Sequence alignment and alpha-helix prediction of nine rhabdovirus glycoproteins in the putative tail region. Shown are sequences for rabies CVS strain (37), Mokola virus (34), VSV Indiana (VSV-Ind [30]), VSV New Jersey (VSV-NJ [16]), Chandipura virus (25), Piry virus (2), spring viremia of carp virus (SVCV GenBank), sigma virus (33), and infectious hematopoietic necrosis virus (IHNV [23]). Shaded residues show conservative changes; shaded and boldfaced residues indicate conservation. The two large boxes indicate regions where all sequences are rich in predicted alpha helices (4–6, 17). Amino acid numbering corresponds to the protein before signal sequence cleavage. Arrowheads indicate the positions of mutants V392G and M396T; arrows indicate the insertion mutants described by Li et al. (24).

398 may act as a hinge during the structural transitions of G. Interestingly, insertion mutants in this region of VSV G (Fig. 5) abolish its fusion activity (24). It is possible that these insertions, by stabilizing the I state, do not allow G to acquire its native structure at the cell surface. Alternatively, this region may also regulate the transition toward the fusogenic conformation of G (which is different from the I conformation). Whatever the case, the results of Li et al. (24) and those presented in this report suggest that this region plays a key role in the control of rhabdovirus glycoprotein conformational changes.

Because of the ability of the MAbs 17A4 and 29EC2 to select mutants for which the conformational transition from N to I state is affected, we would have expected to select more mutants involving different regions of the protein. For example, in the case of influenza virus hemagglutinin, many different mutations have been shown to affect the characteristics of the low-pH-induced structural transition (10). However, despite many cycles of selection on several clonal populations of CVS (28), we repeatedly obtained the same mutations at positions 44, 392, and 396 (E282K has been obtained only once). If, as proposed previously (21), the role of the I state is to avoid fusion in the Golgi apparatus, mutations which would significantly alter the equilibrium between the N and the I state would be highly unfavorable. For example, an excessive stabilization of the N state would lead to undesirable fusion in the Golgi apparatus. Alternatively, we cannot exclude the possibility that such mutants would be unable to induce membrane fusion.

Another result of this study is the presence of a hexagonal lattice of glycoprotein molecules at the surface of mutants M44I and V392G. This lattice is stabilized in the cold and at pH 6.6, which corresponds to prefusion conditions (12, 19). Interestingly, the lattice is detectable at the surface of mutants with a lesser tendency to aggregate, which suggests that lattice formation may compete with aggregation. Although the exact significance of this lattice is unknown, these results demonstrate the ability of the spikes to interact laterally, most probably via their ectodomain.

The lattice at the viral surface is most pronounced at the surface of M44I, a mutant which exhibits strong cooperativity in the conformational change. Together with the fact that the lattice is disrupted during the structural transition toward the I state, this finding suggests that the interactions between the spikes which are responsible for lattice formation stabilize the glycoprotein in its N or A conformation and may be the cause of the cooperativity of the conformational change toward the I state. If lateral interactions stabilize the N state, the difference between the mutants and the parental strain might also be

explained by a difference in the glycoprotein density at the viral surface. This is most probably not the case because the numbers of G protein per virus particle were similar with all mutants, as judged by sodium dodecyl sulfate-polyacrylamide gel electrophoresis (not shown). Lateral interactions between glycoproteins may be important during the budding process and would help to explain the entrapment activity of G protein alone, as recently described for G protein expressed from an alphavirus vector (29). Alternatively, these interactions may also play an important role in the fusion mechanism, in view of the results suggesting that more than one spike is involved in formation of the fusion site for both VSV and rabies virus (3, 19).

ACKNOWLEDGMENT

This work was supported by the CNRS (UPR 9053).

REFERENCES

- Benmansour, A., H. Leblois, P. Coulon, C. Tuffereau, Y. Gaudin, A. Flamand, and F. Lafay. 1991. Antigenicity of rabies virus glycoprotein. *J. Virol.* **65**:4198–4203.
- Brun, G., X. K. Bao, L. Prevec. 1995. The relationship of Piry virus to other vesiculoviruses: a re-evaluation based on the glycoprotein gene sequence. *Intervirology* **38**:274–282.
- Bundo-Morita, K., S. Gibson, and J. Lenard. 1988. Radiation inactivation analysis of fusion and hemolysis by vesicular stomatitis virus. *Virology* **163**:622–624.
- Chou, P. Y., and G. D. Fasman. 1974. Conformational parameters for amino acids in helical, β -sheet and random coil regions. *Biochemistry* **13**:211–222.
- Chou, P. Y., and G. D. Fasman. 1974. Prediction of protein conformation. *Biochemistry* **13**:222–245.
- Chou, P. Y., and G. D. Fasman. 1977. β -Turns in proteins. *J. Mol. Biol.* **115**:135–175.
- Clague, M. J., C. Schoch, L. Zech, and R. Blumenthal. 1990. Gating kinetics of pH-activated membrane fusion of vesicular stomatitis virus with cells: stopped-flow measurements by dequenching of octadecylrhodamine fluorescence. *Biochemistry* **29**:1303–1308.
- Cox, J. H., B. Dietzschold, and L. G. Schneider. 1977. Rabies virus glycoprotein. *Infect. Immun.* **16**:754–759.
- Crimmins, D. L., W. B. Mehard, and S. Schlesinger. 1983. Physical properties of a soluble form of the glycoprotein of vesicular stomatitis virus at neutral and acidic pH. *Biochemistry* **22**:5790–5796.
- Daniels, R. S., J. C. Downie, A. J. Hay, M. Knossow, J. J. Skehel, M. L. Wang, and D. C. Wiley. 1985. Fusion mutants of the influenza virus hemagglutinin glycoprotein. *Cell* **40**:431–439.
- Doms, R. W., D. S. Keller, A. Helenius, and W. Balch. 1987. Role for adenosine triphosphate in regulating the assembly and transport of vesicular stomatitis virus G protein trimers. *J. Cell Biol.* **105**:1957–1969.
- Durrer, P., Y. Gaudin, R. W. H. Ruigrok, R. Graf, and J. Brunner. 1995. Photolabeling identifies a putative fusion domain in the envelope glycoprotein of rabies and vesicular stomatitis viruses. *J. Biol. Chem.* **270**:17575–17581.
- Flamand, A., H. Raux, Y. Gaudin, and R. W. H. Ruigrok. 1993. Mechanism of rabies virus neutralization. *Virology* **194**:302–313.
- Fredericksen, B. L., and M. A. Whitt. 1995. Vesicular stomatitis virus glycoprotein mutations that affect membrane fusion activity and abolish virus

- infectivity. *J. Virol.* **69**:1435–1443.
15. **Fredericksen, B. L., and M. A. Whitt.** 1996. Mutations at two conserved acidic amino acids in the glycoprotein of vesicular stomatitis virus affect pH-dependent conformational changes and reduce the pH threshold for membrane fusion. *Virology* **217**:49–57.
 16. **Gallione, C. J., and J. K. Rose.** 1983. Nucleotide sequence of a cDNA clone encoding the entire glycoprotein from the New Jersey serotype of vesicular stomatitis virus. *J. Virol.* **46**:162–169.
 17. **Garnier, J., D. J. Osguthorpe, and B. Robson.** 1978. Analysis of accuracy and implications of simple methods for predicting the secondary structure of globular proteins. *J. Mol. Biol.* **120**:97–120.
 18. **Gaudin, Y., R. W. H. Ruigrok, and J. Brunner.** 1995. Low-pH induced conformational changes in viral fusion proteins: implications for the fusion mechanism. *J. Gen. Virol.* **76**:1541–1546.
 19. **Gaudin, Y., R. W. H. Ruigrok, M. Knossow, and A. Flamand.** 1993. Low-pH conformational changes of rabies virus glycoprotein and their role in membrane fusion. *J. Virol.* **67**:1365–1372.
 20. **Gaudin, Y., R. W. H. Ruigrok, C. Tuffereau, M. Knossow, and A. Flamand.** 1992. Rabies virus glycoprotein is a trimer. *Virology* **187**:627–632.
 21. **Gaudin, Y., C. Tuffereau, P. Durrer, A. Flamand, and R. W. H. Ruigrok.** 1995. Biological function of the low-pH, fusion-inactive conformation of rabies virus glycoprotein (G): G is transported in a fusion-inactive state-like conformation. *J. Virol.* **69**:5528–5534.
 22. **Gaudin, Y., C. Tuffereau, D. Segretain, M. Knossow, and A. Flamand.** 1991. Reversible conformational changes and fusion activity of rabies virus glycoprotein. *J. Virol.* **65**:4853–4859.
 23. **Koener, J. F., C. W. Passavant, G. Kurath, and J. Leong.** 1987. Nucleotide sequence of a cDNA clone carrying the glycoprotein gene of infectious hematopoietic necrosis virus, a fish rhabdovirus. *J. Virol.* **61**:1342–1349.
 24. **Li, Y., C. Drone, E. Sat, and H. P. Ghosh.** 1993. Mutational analysis of the vesicular stomatitis virus glycoprotein G for membrane fusion domains. *J. Virol.* **67**:4070–4077.
 25. **Masters, P. S., R. S. Bhella, M. Butcher, B. Patel, H. P. Ghosh, and A. K. Banerjee.** 1989. Structure and expression of the glycoprotein gene of Chandipura virus. *Virology* **171**:285–290.
 26. **Préhaud, C., P. Coulon, F. Lafay, C. Thiers, and A. Flamand.** 1988. Antigenic site II of the rabies virus glycoprotein: structure and role in viral virulence. *J. Virol.* **62**:1–7.
 27. **Puri, A., S. Grimaldi, and R. Blumenthal.** 1992. Role of viral envelope sialic acid in membrane fusion mediated by the vesicular stomatitis virus envelope glycoproteins. *Biochemistry* **31**:10108–10113.
 28. **Raux, H., P. Coulon, F. Lafay, and A. Flamand.** 1995. Monoclonal antibodies which recognize the acidic configuration of the rabies glycoprotein at the surface of the virion can be neutralizing. *Virology* **210**:400–408.
 29. **Rolls, M. M., P. Webster, N. H. Balba, and J. K. Rose.** 1994. Novel infectious particles generated by expression of the vesicular stomatitis virus glycoprotein from a self-replicating RNA. *Cell* **79**:497–506.
 30. **Rose, J. K., and C. J. Gallione.** 1981. Nucleotide sequences of the mRNAs encoding the vesicular stomatitis virus G and M proteins determined from cDNA clones containing the complete coding regions. *J. Virol.* **39**:519–528.
 31. **Seif, I., P. Coulon, P. E. Rollin, and A. Flamand.** 1985. Rabies virulence: effect on pathogenicity and sequence characterization of rabies virus mutations affecting antigenic site III of the glycoprotein. *J. Virol.* **51**:505–514.
 32. **Struck, D. C., D. Hoekstra, and R. E. Pagano.** 1981. Use of resonance energy transfer to monitor membrane fusion. *Biochemistry* **20**:4093–4099.
 33. **Teninges, D., and F. Bras-Herregg.** 1987. Rhabdovirus sigma, the hereditary CO₂ sensitivity agent of *Drosophila*: nucleotide sequence of a cDNA clone encoding the glycoprotein. *J. Gen. Virol.* **68**:2625–2638.
 34. **Tordo, N., H. Bourhy, S. Sather, and R. Olo.** 1993. Structure and expression in baculovirus of the Mokola virus glycoprotein: an efficient recombinant vaccine. *Virology* **194**:59–69.
 35. **Whitt, M. A., L. Buonocore, C. Prehaud, and J. K. Rose.** 1991. Membrane fusion activity, oligomerization, and assembly of the rabies virus glycoprotein. *Virology* **185**:681–688.
 36. **Wunner, W. H., K. J. Reagan, and H. Koprowski.** 1984. Characterization of saturable binding sites for rabies virus. *J. Virol.* **50**:691–697.
 37. **Yelverton, E., S. Norton, J. F. Obijeski, and D. V. Goeddel.** 1983. Rabies virus glycoprotein analogs: biosynthesis in *E. coli*. *Science* **219**:614–620.
 38. **Zhang, L., and H. P. Ghosh.** 1994. Characterization of the putative fusogenic domain in vesicular stomatitis virus glycoprotein G. *J. Virol.* **68**:2186–2193.